

## Modeling for Taxol<sup>®</sup> Separation in a Simulated Moving Bed

Marco Aurelio Cremasco\* and Axel Nicolas Starquit

Faculdade de Engenharia Química; Universidade Estadual de Campinas; Barão Geraldo; 13083-970; Campinas - SP - Brasil

### ABSTRACT

*This work presents an alternative numerical resolution strategy for a model to describe the dynamic of linear adsorption processes involving multicomponent mixture of taxanes with Taxol<sup>®</sup> (paclitaxel), a powerful anti-cancer agent, and non-identified impurities, in a Simulated Moving Bed (SMB) system. To solve the model, a hybrid method were used. The liquid concentration inside the particles was found analytically and was related with the liquid bed concentration using Duhamel's theorem. The results from simulation were compared with experimental ones from the literature, showing a good agreement, which demonstrated the applicability of the model and of the hybrid resolution proposed.*

**Key words:** Cancer, Taxol, Simulated moving bed, Computer simulation, Multicomponent separation

### INTRODUCTION

Cancer is a public health concern worldwide that must be considered in various area of the knowledge. In USA, appear a million cases each year. In the South East of the Brazil, cancer is the second largest cause of death. The introduction of chemotherapy to combat the cancer results in significant tumors cure that didn't control with success by exclusive use of surgery and/or radiotherapy (Bonadonna, 1990). Researchers around the world have particular attention in the study of natural products as possible source of antineoplastic agents. Due to the diversity of the chemical structures found in theses products, there are big chances to identify news molecules with anti-tumor activities. The Taxol<sup>®</sup> (commercial name for Paclitaxel) discovery offers good points for this reasoning (Holanda et al., 2008).

According to Rhoads (1995), while many drugs act to disrupt the cancer cells, Taxol<sup>®</sup> paralyzes the internal structure. In the metaphase stage of cell replication, chromosome pairs split and move to the opposite ends of the cell and wait to become part of a daughter cell. Rhoads (1995) reported that these chromosomes were guided by the microtubules made of tubulin. These bundles of microtubules must be dismantled before the cell be divided. However, Taxol<sup>®</sup> prevents the cells from dividing further and essentially halts the cancer growth. It has been approved by the FDA, in the USA, for the treatment of advanced breast cancer, lung cancer, and refractory ovarian cancer. Taxol<sup>®</sup> is a diterpene compound (Fig. 1). It has the molecular formula  $C_{47}H_{51}NO_{14}$ , with molecular weight 853.92.

Taxol<sup>®</sup> is an extremely hydrophobic molecule. Its low solubility in water makes the administration of

\* Author for correspondence: cremasco@feq.unicamp.br

the drug difficult. However, it can be administered by dissolving in a cremaphore, alcohol, castor oil, and saline solution. The complexity of Taxol® rests primarily in its stereochemistry, which makes organic synthesis extremely difficult (Wu, 1999). Taxol® can be isolated from the bark of the Pacific yew (*Taxus brevifolia*). It also can be produced and recovered from the plant tissue culture (PTC) broth (Srinivasan, 1994).

The presence of a number of structurally similar compounds in the source material for Taxol®, such as cephalomannine and baccatin, complicates the recovery and purification process (Wu, 1999). Over 100 compounds with taxane skeleton have been isolated. A major portion of the purification cost is due to the separation of Taxol® from a

large number of taxanes with similar molecular structures. In this case, Taxol® separation and purification usually involves extraction, solvent partitioning, and preparative HPLC purification to eliminate the hazardous solvents and the expense associated with pressure equipment (Wu, 1999). Conventional batch chromatography has been used for Taxol® separation from PTC broth (Wu et al., 1997). This technique, however, is expensive and has low yield and low productivity. A simulated moving bed (SMB), which saves solvent and increases the adsorbent utilization (Borges da Silva et al., 2006), can result in a more economical separation process. In a traditional SMB system, a series of fixed bed columns is connected to form a circuit (Fig. 2).

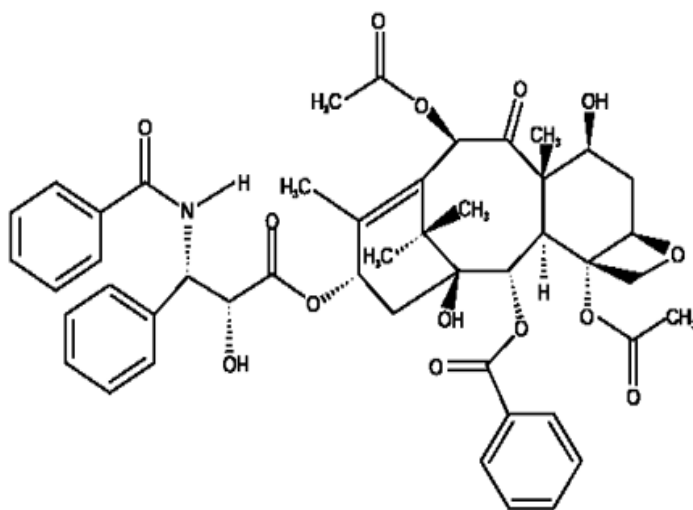


Figure 1 - Chemical structure of Taxol®.

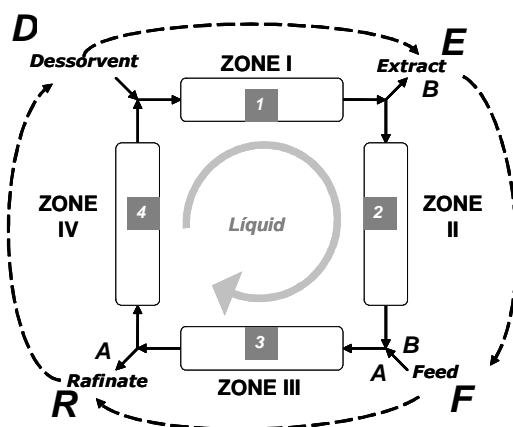


Figure 2 - Classical four zones SMB system.

This circuit is divided into four zones by two inlet ports (feed and a solvent) and two outlet ports (a raffinate port, where the low-affinity mixture A is removed, and an extract port, where a high-affinity mixture B is removed). The inlet and outlet ports are periodically moved along the solvent flow direction by multiple-position valves, causing an apparent countercurrent movement between the liquid and the solid phase. As in batch chromatography, mixture A migrates faster than mixture B in the liquid flow direction.

If the average feed port velocity is lower than the mixture A migration velocity and larger than mixture B migration velocity, then A will have a net velocity in the solvent flow direction relative to the feed port, while B will have a net velocity in the opposite direction. In this case, the standing wave theory says that mixture A adsorption wave remains stationary in zone IV, while its desorption wave stands in zone II. Solute B adsorption wave lies in zone III, adsorption wave lies in zone III, and its desorption wave stands in zone I, as represented in Figure 2. In this Figure, A, means low-affinity mixture; B, high-affinity mixture; D means solvent flow; E, extract flow; F, feed flow; and R, raffinate flow.

Due to the complexity of the SMB process, simulations are necessary at many stages in the development of a specific application. To perform such simulations, several models from literature (Ching et al., 1994) can be used. There are two main approaches to the modeling of an SMB. In the first one the SMB is represented by an equivalent true moving bed (Ching et al., 1991; Lu and Ching, 1997; Lehoucq et al., 2000). This approach results in a set of ordinary differential equations that results in a mathematical problem, and lost information about intrinsic dynamic behavior of the SMB, limiting the understanding process and the application of those models for process control (Dünnebier et al., 1998).

The second approach consists of a dynamic modeling, which considers separately each column and the real successive switch positions in the process. In this case, a chromatographic model is chosen for each individual of SMB column. With the ideal plug flow model, an analytical solution was proposed (Zhong and Guiochon, 1996), but the results pointed that mass transfer effects can not be, in many practical applications, neglected, so numerical simulations were indispensable. A fast and accurate resolution scheme, using a closed-form solution, was proposed by Dünnebier

et al. (1998). However, when a general rate model is used to represent the mass transfer in each column, almost all authors use the orthogonal collocation technique to solve the problem (Ching et al., 1991; Mallmann et al., 1998; Toumi et al., 2003; Yu and Ching, 2003).

The aim of this work was to develop an alternative numerical resolution strategy for the dynamic prevision of linear adsorption processes in a multicomponent SMB system, using a general rate model.

An adsorption process evolution was computationally determined for a system containing compound mixture, using a hybrid method. Based on Cremasco et al. (2003), the liquid concentration inside the particles was found analytically and it was related with the liquid bed concentration using Duhamel's theorem. The solution for the liquid bed concentration was found numerically, instead of analytically. The results from the hybrid resolution were compared with the experimental ones from literature.

## THEORY

The modeling strategy chosen to represent the SMB process consisted of a dynamic modeling, where each column was modeled individually by a general rate model. In order to obtain this mathematical model, some assumptions must be made: the flow rates are constant in each zone; the transversal cross section is constant for and through column; radial dispersion can be neglected; the axial dispersion coefficient is a function of solute and flow rate; the external mass transfer resistance is considered; solid phase is composed of small spheres of uniform radius; the mobile phase is a dilute solution, so that Henry's law can be used to describe the sorbate uptake; the pore diffusion model describes the intra-particle transport mechanism; no chemical reaction occurs; initial concentration inside the column (liquid and resin) is zero. Based on the previous hypotheses, the adsorption process can be described by the following set of equations, for each solute in each column.

### Solid Phase

$$\varepsilon_p \cdot \frac{\partial q_j^i}{\partial t} + (1 - \varepsilon_p) \cdot \frac{\partial C_p^j}{\partial t} = \varepsilon_p \cdot D_p^j \cdot \frac{1}{r^2} \cdot \frac{\partial}{\partial r} \left( r^2 \cdot \frac{\partial q_j^i}{\partial r} \right) \quad (1)$$

$$C_p^j = k_p^j \cdot q_j^i \quad (2)$$

where  $q$  is the solute concentration in the liquid phase inside the particle pores (volume fraction  $\varepsilon_p$ ),  $C_p$  is the solute concentration on the solid (volume fraction  $1-\varepsilon_p$ ), and indices  $i$  and  $j$ , refer to column and solute, respectively.

#### Fluid Phase

$$\frac{\partial C_j^i}{\partial t} = E_{bj}^i \cdot \frac{\partial^2 C_j^i}{\partial z^2} - u^i \cdot \frac{\partial C_j^i}{\partial z} - Ra_j^i \quad (3)$$

where  $C$  is the solute concentration in the fluid phase (volume fraction  $\varepsilon$ ), and  $Ra$  is the rate of adsorption/desorption of solute by the solid, by reactor volume unit, which is expressed as

$$Ra_j^i = \frac{1-\varepsilon}{\varepsilon} \cdot \frac{3}{R^3} \cdot \frac{\partial}{\partial t} \left\{ \int_0^R [\varepsilon_p \cdot q_j^i + (1-\varepsilon_p) \cdot Cp_j^i] r^2 \cdot dr \right\} \quad (4)$$

Using equation (2) in (1) and (4), results in:

$$[\varepsilon_p + (1-\varepsilon_p) \cdot k_p^j] \frac{\partial q_j^i}{\partial t} = \varepsilon_p \cdot D_p^j \cdot \left( \frac{2}{r} \cdot \frac{\partial q_j^i}{\partial r} + \frac{\partial^2 q_j^i}{\partial r^2} \right) \quad (5)$$

$$Ra_j^i = \frac{1-\varepsilon}{\varepsilon} \cdot \frac{3}{R^3} \cdot [\varepsilon_p + (1-\varepsilon_p) \cdot k_p^j] \frac{\partial}{\partial t} \left\{ \int_0^R q_j^i \cdot r^2 \cdot dr \right\} \quad (6)$$

The initial and boundary conditions that describe the adsorption process are expressed as follows

$$C_j^i = q_j^i = 0 \quad \text{for } t = 0 \quad (7)$$

$$\frac{\partial q_j^i}{\partial r} = 0 \quad \text{for } r = 0 \quad (8)$$

$$q_j^i = C_j^i \quad \text{for } r = R \quad (9)$$

$$\frac{\partial C_j^i}{\partial z} = 0 \quad \text{for } z = L_C \quad (10)$$

$$\frac{\partial C_j^i}{\partial z} = \frac{u^i}{E_{bj}^i} \cdot (C_j^i - C_{0j}^i) \quad \text{for } z = 0 \quad (11)$$

$C_{0j}^i$  in Eq. (11) is the solute concentration in the column inlet flow, which depends on the system evolution as shown in Eqs. (12); and:

for the column next to the feed port

$$C_{0III}^i = \frac{Q_{II} \cdot C_{II}^i \Big|_{z=L_{II}} + Q_F \cdot C_F^i}{Q_{III}} \quad (12a)$$

for the column next to the solvent port

$$C_{0I}^i = \frac{Q_{IV}}{Q_I} \cdot C_{IV}^i \Big|_{z=L_{IV}} \quad (12b)$$

for the other columns

$$C_{0j}^i = C_{j-1}^i \Big|_{z=L_C} \quad (12c)$$

Most of the parameters necessary for the simulations were estimated using the correlations from the literature. The effective diffusion coefficient was obtained by experimental information or from literature (Mackie and Meares, 1955):

$$D_p^i = \frac{\varepsilon_p}{(2-\varepsilon_p)^2} D_{AB}^i \quad (13)$$

The convective mass transfer coefficient is calculated by (Wilson and Geankoplis, 1966),

$$Sh_j^i = \frac{1.09}{\varepsilon} \left( Pe_{MP}^{1/3} \right)_j^i \quad (14)$$

with Sherwood number and molecular mass Peclet number for a particle defined by, respectively:

$$Sh_j^i = \frac{2k_{fj}^i R_p}{D_{AB}^i} \quad (15)$$

$$Pe_{MPj}^i = \frac{2u_j \varepsilon R_p}{D_{AB}^i} \quad (16)$$

and the axial dispersion coefficient calculated from (Athalye, 1992),

$$\frac{E_{bj}^i}{2u_j \varepsilon R_p} = \left[ \left( \frac{Pe_{MP}}{1-\varepsilon} \right)^{1/6} \right]^i \quad (17)$$

## NUMERICAL RESOLUTION

The resolution method used in this work was a hybrid method based on previous work, in which was developed for the prediction of breakthrough curves for the adsorption of a single compound (Cremasco et al., 2003). The intra-particle liquid solute concentration was found analytically and correlated to the liquid bed concentration through Duhamel's theorem. The use of this theorem resulted in an equation connecting the intraparticle liquid concentration,  $q$ , to the liquid bed concentration,  $C$ . This correlation is expressed as

$$q_j^i = \int_0^t \left[ -\frac{\partial \theta_j^i(r, t - \tau)}{\partial \tau} \right] \cdot C_j^i \cdot d\tau \quad (18)$$

where  $\theta$  is the dimensionless solution of the problem established by Eq. (5), initial condition (7), and boundary conditions (8) and (9);  $t$ , is time, and  $\tau$ , the integrating variable. However, in order to express  $Ra$ , it is more convenient to use the average concentration,  $\bar{\theta}$ , defined as (Cremasco, 1998)

$$\bar{\theta}_j^i(t) = \frac{3}{R^3} \cdot \int_0^R \theta_j^i(r, t) \cdot r^2 \cdot dr \quad (19)$$

Substituting the analytic solution into the previous equation results in:

$$\bar{\theta}_i^j(t) = 1 - 6 \sum_{n=1}^{\infty} \frac{1}{\gamma_n^2} \cdot \frac{(Bi_{Mj}^i)^2}{[\gamma_n^2 - Bi_{Mj}^i(Bi_{Mj}^i - 1)]} \cdot e^{-\gamma_n^2 \cdot Fo_M^i} \quad (20)$$

were the modified Fourier mass number, molecular Biot number, and  $\gamma_n$  are defined by:

$$Fo_M^i = \frac{\epsilon_p}{[\epsilon_p + (1 - \epsilon_p)k_p^i]} \frac{D_p^i t}{R_p^2} \quad (21)$$

$$Bi_{Mj}^i = \frac{R_p \cdot k_{fj}^i}{k_p^i \cdot D_p^i} \quad (22)$$

$$\frac{\gamma_n}{\tan(\gamma_n)} = 1 - Bi_{Mj}^i \quad (23)$$

Using the average concentration,  $\bar{\theta}$ , and Duhamel's theorem, Eq. (6) can be rearranged to obtain

$$Ra_j^i = [\epsilon_p + (1 - \epsilon_p)k_p^i] \frac{\partial}{\partial t} \left\{ \int_0^t \frac{d}{d\xi} \bar{\theta}_j^i(\xi) \Big|_{\xi=t-\tau} C_j^i(z, \tau) \cdot d\tau \right\} \quad (24)$$

The Eq. (24) is introduced into Eq. (3), which is numerically solved by a first-order discretization method. As result, linear tridiagonal sets of equations have to be solved, which is accomplished using the Thomas' algorithm. All algebraic sets of equations have to be solved simultaneously in order to calculate the column entrance concentration in the next time step using of Eqs. (12). To do so, it is easier to work with a fixed time integration step,  $\Delta t$ , and a calculated spatial step,  $\Delta z_j^i$ . Also, in the physical process, one can assume that the past concentration in the column will not influence the rate of adsorption at the actual time. Mathematically, the derivative in Eq. (24) tends to zero when  $\tau$  tends to zero. For this reason, the integral in this equation is estimated using calculated values from the beginning of the past switching period, until the actual time. This allows us to diminish the computing time and the memory used. Note also that at each switching there will be a change in the position of the columns in the system (zone), and that their boundary conditions are continuously changing.

## RESULTS AND DISCUSSION

Numerical results were obtained for Taxol® separation from three impurities in a four zones SMB, each zone being composed of one column. The physical parameters of the solutes are presented in Table 1, while the different operating conditions explored in the experiments and simulations are summarized in Table 2. The simulated curves were confronted with the experimental ones. The average experimental solute concentrations in each collected sample were determined from HPLC. The experimental, and computational, elution curves were based on the average product concentration, where each data point was taken at an interval of time equal to  $t_{switch}/2$ .

The comparisons are presented in Figures 3 and 4 for Run 1 and 2 respectively, Figures 5 and 6 show the solutes concentration distributions in the mass-transfer zones at the cyclic-steady state.

**Table 1** - Taxanes partition and diffusion coefficients (Cremaşco et al., 2009).

| Taxanas    | Tr10  | Taxol@ | Tr18  | Tr21  |
|------------|-------|--------|-------|-------|
| $k_p$ (-)  | 82.52 | 40.03  | 38.67 | 15.09 |
| * $D_{AB}$ | 2.569 | 2.560  | 2.564 | 2.526 |
| * $D_p$    | 1.310 | 0.590  | 0.920 | 0.384 |

( $10^{-4} \text{ cm}^2/\text{min}$ )

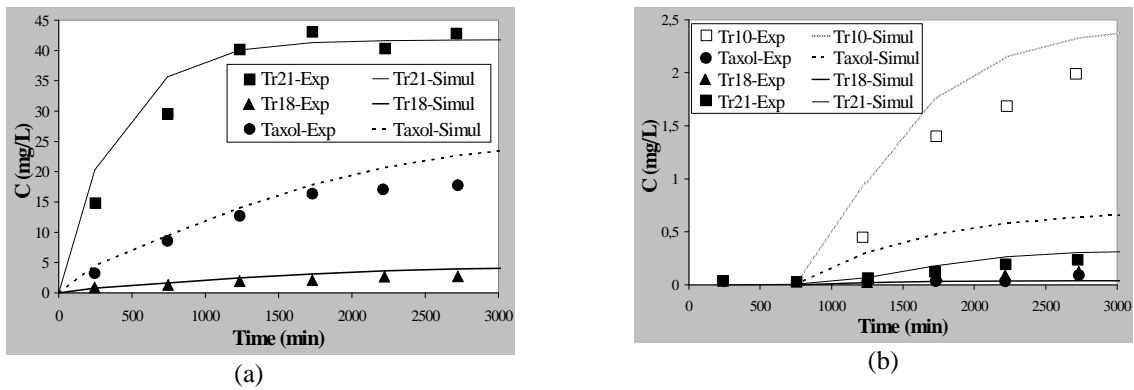


**Figure 3** - Comparison of average experimental data and simulation results, for Run 1: (a) Raffinate; (b) Extract.

**Table 2** - Feed composition and SMB operating parameters (Cremaşco et al. 2009).

| Parameter | $C_{\text{Paclitaxel}}^F$<br>(mg/L) | $C_{\text{Tr18}}^F$<br>(mg/L) | $C_{\text{Tr21}}^F$<br>(mg/L) | $C_{\text{Tr10}}^F$<br>(mg/L) | $Q^I$<br>(ml/min) | $Q^{II}$<br>(ml/min) | $Q^{III}$<br>(ml/min) | $Q^{IV}$<br>(ml/min) | $t_{\text{switch}}$<br>(min.) |
|-----------|-------------------------------------|-------------------------------|-------------------------------|-------------------------------|-------------------|----------------------|-----------------------|----------------------|-------------------------------|
| Run 1     | 120.8                               | 19.6                          | 192.3                         | 14.4                          | 1.808             | 0.906                | 1.070                 | 0.322                | 494.4                         |
| Run 2     | 22.3                                | 3.92                          | 31.35                         | -                             | 1.711             | 0.626                | 0.994                 | 0.415                | 320.5                         |

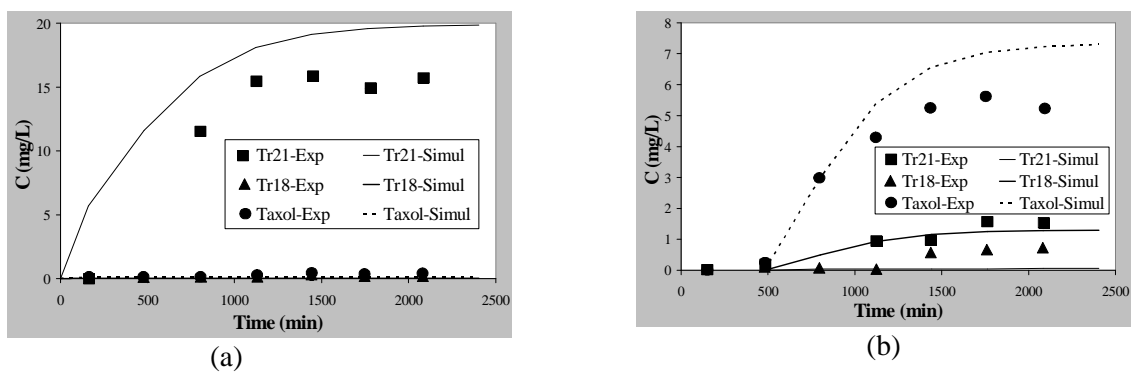


**Figure 4** - Comparison of average experimental data and simulation results, for Run 2: (a) Raffinate; (b) Extract.

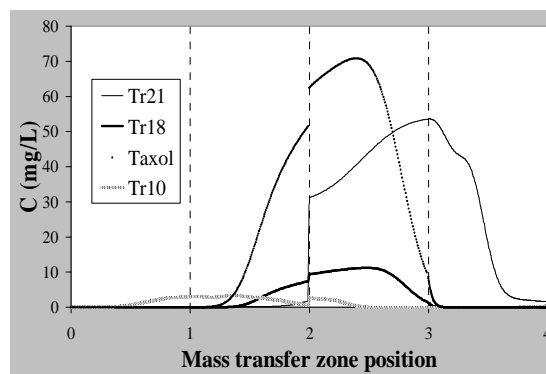


**Figure 5** - Simulated curves of solutes concentration distribution along mass-transfer at the cyclic-steady state, for Run 1.

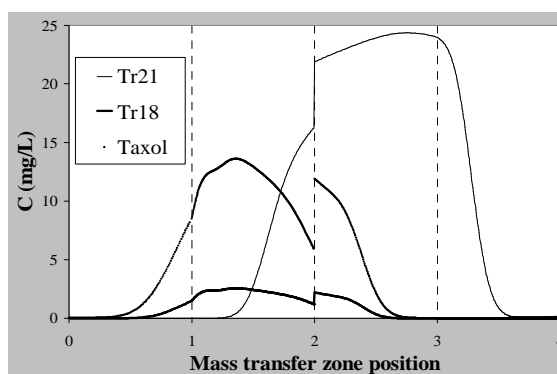


**Figure 6** - Simulated curves of solutes concentration distribution along mass-transfer at the cyclic-steady state, for Run 2. Figure 6- Simulated curves of solutes concentration distribution along mass-transfer at the cyclic-steady state, for Run 2.

Figure 3a showed that after switching three times the valves position, the Tr21 was already reaching the cyclic steady-state in the raffinate. At the cyclic steady-state, the average concentration was constant along the time. For the two other compounds present in the raffinate, the experimental result seemed to attain the cyclic steady-state before the end of the experiment. Yet, the simulated curve did not arrive at the cyclic steady-state. In Figure 3b, only the Tr10 did not attain the cyclic steady-state. In the extract, almost all the numerical curves were above the experimental results. Those discrepancies might be due to some deviation of the parameter from the values presented in Table 1, due to some imprecision in the determination of those parameters. It could also be possible that the deviation between experimental and simulated results were due to flow rates deviation from the

values presented in Table 2, due to the limitation imposed by the pump precision.

Figure 4 showed that the simulated curves (Fig. 3 and 4) acceptably predicted the overall SMB behavior. Note that the experimental precision are not presented in Figures 3 and 4 because they are not known, so that they might also explain the discrepancies between the simulated and experimental results. These results were obtained in 83 and 65 min for Run 1 and Run 2, respectively.

Figures 5 and 6 were obtained through the simulation's results. Figure 5 showed that desorption waves of Taxol<sup>®</sup>, Tr21 e Tr18 were in zone II. Tr21 adsorption wave was in zone IV, while Tr18 and Taxol<sup>®</sup> adsorption waves were in between zone III and IV, for Tr10, the adsorption wave was in zone III and desorption wave in zone I. The possible flow rates imprecision could

explain the deviation of the result from the expected curves, where Tr18 and Taxol<sup>®</sup> adsorption waves should remain in zone IV. In Figure 6, all the adsorption and desorption waves were in the zone where they were expected by the standing wave theory, showing that the separation occurred properly.

## CONCLUSIONS

The hybrid method for the numerical simulation of SMB presented in this paper, offered satisfactory predictive results in a short time in comparison to the physical separation process. Still, discrepancies between the theoretical and experimental curves appeared. These were most likely due to some experimental errors, which might be deviation of the flow rates from the expected ones, or imprecision in the mass-transfer and equilibrium parameters. The main limitation of this approach was the fact that Duhamel's theorem was only applicable to linear PDE with linear initial and boundary conditions. On the other hand, the comparison between the experimental and model results indicated that the method was efficient and easy to apply, solving the problem in a very short computational time to a complex mixture separation process, such as SMB technique and taxanes mixture.

## ACKNOWLEDGMENT

The authors acknowledge the financial support obtained from the Sao Paulo State Research Foundation (FAPESP – n. 01/08101-3) for this research project.

## RESUMO

O Taxol<sup>®</sup>, conhecido também como Paclitaxel, é uma droga poderosa utilizada no tratamento de câncer. Quanto à sua obtenção, o Taxol<sup>®</sup> pode ser recuperado a partir de um meio líquido cultivado, oriundo da cultura de células vegetais. Entretanto, o Taxol<sup>®</sup> existe em mistura com um número alto de taxanas estruturalmente semelhantes a ele, o que leva a dificuldade em recuperá-lo.

Uma das estratégias tecnológicas mais recentes para este tipo de situação é o emprego de sistemas cromatográficos contínuos conhecidos como Leito

Móvel Simulado (LMS). O LMS caracteriza-se por provocar o aparente escoamento contínuo em contracorrente entre a fase líquida e o leito sólido, aumentando a força motriz necessária para transferência de massa e, conseqüentemente, a eficiência do processo. Dessa maneira, o objetivo deste trabalho é o de apresentar um modelo matemático e a sua solução visando à separação de Taxol<sup>®</sup> (Paclitaxel) de uma mistura de taxanas. O método matemático proposto é híbrido, em que a fase estacionária é resolvida analiticamente, enquanto a fase móvel, via resolução numérica, sendo ambas as fases interconectadas pelo teorema de Duhamel. Os resultados oriundos da solução numérica foram comparados com aqueles experimentais encontrados na Literatura, demonstrando desempenho bastante favoráveis para o modelo e métodos de solução propostos.

## NOTATION

- $C_b$  - solute concentration in the mobile phase,  $ML^3$ ;
- $C_p$  - intra-particle liquid phase concentration,  $ML^3$ ;
- $C_0$  - column injection concentration,  $ML^3$ ;
- $D$  - column diameter, L;
- $D_{AB}$  - free diffusion coefficient,  $L^2T^{-1}$ ;
- $D_p$  - effective diffusion coefficient,  $L^2T^{-1}$ ;
- $E_b$  - axial dispersion coefficient,  $L^2T^{-1}$ ;
- $k_f$  - convective mass transfer coefficient,  $LT^{-1}$ ;
- $k_p$  - equilibrium partition constant, -;
- $L_c$  - single column length, L;
- $q$  - superficial solid intra-particle concentration,  $ML^3$ ;
- $R_p$  - average particle radius, L;
- $t_{switch}$  - switching period, T;
- $u$  - SMB liquid interstitial velocity,  $LT^{-1}$ .

### Greek letters

- $\varepsilon$  - bed porosity, -;
- $\varepsilon_p$  - particle porosity, -;
- $\theta$  - dimensionless concentration, -.

### Subscripts and superscripts

- E - extract;
- F - feed;
- i - specie i;
- j - zone j;
- R - raffinate;
- S - solvent;
- I - zone I;

- II - zone II;  
 III - zone III;  
 IV - zone IV.

## REFERENCES

- Athalye, A.M., Gibbs, S.J., and Lightfoot, E.N. (1992), Predictability of chromatographic protein separations: Study of size-exclusion media with narrow particle size distribution. *J. Chrom.*, **589**, 71-85.
- Bonadonna, G. (1990), Does chemotherapy fulfill its expectation in cancer treatment? *Ann. Oncol.*, **1**, 11-21.
- Borges da Silva, A. A., Ulson de Souza, A. A., Rodrigues, A. E.; Ulson de Souza, and S. M. A. (2006), Glucose isomerization in simulated moving bed reactor by *Glucose isomerase*. *Braz. Arch. Biol.*, **49** (3), 491 – 502.
- Ching, C.B., Chu, K.H., Hidajat, K., and Uddin, M.S. (1991), Experimental and modeling studies of the transient Behavior of a simulated countercurrent adsorber. *J. Chem. Eng. Japan*, **24** (5), 614-621.
- Cremasco, M. A. (1998), Mass-transfer Fundamentals. Editora da Unicamp, Campinas, pp. 251-312.
- Cremasco, M.A., Guirardello, R., and Wang, N.-H.L. (2003), Adsorption of aromatic amino acid in a fixed bed column. *Brazilian J. Chem. Eng.*, **20** (3), 327-334.
- Cremasco, M.A., Hritzko, B.J., and Wang, N.-H. L. (2009), Experimental purification of paclitaxel from a complex mixture of taxanes using a simulated moving bed. *Brazilian J. Chem. Eng.*, **26** (1), 207-218.
- Dünnebier, G., Weirich, I., and Klatt, K.-U. (1998), Computationally efficient dynamic modeling and simulation of simulated moving bed chromatographic processes with linear isotherms. *Chem. Eng. Sci.*, **53** (14), 2537-2546.
- Holanda, C. M. C. X., Oliveira, H. E., Rocha, L. G., Spyrides, M. H. C., Aragão, C. F. S., and Medeiros, A. C. (2008), Effect of Paclitaxel (Taxol®) on the Biodistribution of Sodium Pertechnetate ( $\text{Na}^{99\text{m}}\text{TcO}_4$ ) in Female Wistar Rats. *Braz. Arch. Biol.*, **51** (Special number), 191 – 196.
- Lehoucq, S., Verheve, D., Vande Wouwer, A., and Cavaoy, E. (2000), SMB enantioseparation: process development, modeling, and operating conditions. *AIChE J.*, **46** (2), 247-256.
- Lu, Z.P., and Ching, C.B. (1997), Dynamics of simulated moving-bed adsorption separation *Process. Sep. Sci. Technol.*, **32** (12), 1993-2010.
- Mallmann, T., Burris, B.D., Ma, Z., and Wang, N.H.L. (1998), Standing wave design of nonlinear SMB systems for fructose separation. *AIChE J.*, **44** (12), 2628-2646.
- Rasmuson, A. (1981), Exact solution of a model for diffusion and transient adsorption in particles and longitudinal dispersion in packed beds. *AIChE J.*, **27** (6), 1032-1035.
- Rasmuson, A. (1985), Exact solution of a model for diffusion in particles and longitudinal dispersion in packed beds: Numerical evaluation. *AIChE J.*, **31** (3), 518-519.
- Rosen, J.B. (1952), Kinetics of a fixed bed system for solid diffusion into spherical particles. *J. Chem. Phys.*, **20** (3), 387-394.
- Rhoads, D.N. (1995), The recovery of Taxol from plant tissue culture media. BSc Thesis, Purdue University, West Lafayette, USA.
- Srinivasan, V., Pestchanker, L., Moser, S., Hirasuna, T.J., Taticek, R., and Shuler, M.L., (1994), Taxol production in bioreactors: Kinetics of biomass accumulation, nutrient uptake, and Taxol production by cell suspensions of *Taxus baccata*, *Biotechnol. Bioeng.*, **47**, 666-676.
- Toumi, A., Engell, S., Ludemann-Hombouger, O., Nicoud, R.M., and Bailly, M. (2003), Optimization of simulated moving bed and varicol processes. *J. Chrom. A*, **1006**, 15-31.
- Wilson, E.J., and Geankoplis, C.J. (1966), Liquid mass transfer at very low Reynolds numbers in packed beds, *Ind. Eng. Chem. Fundam.*, **5**, 9-14.
- Wu, D.-J, Ma, Z., Au, B.W. and Wang, N.-H, L. (1997), Recovery and purification of Paclitaxel using low-pressure liquid chromatography, *AIChE J.*, **3** (1), 232-242.
- Wu, D.-J. (1999), Development of simulated moving bed chromatography processes for biochemical purification. PhD Thesis, Purdue University, West Lafayette, USA.
- Yu, H.W., and Ching, C.B. (2003), Modeling, simulation and operation performance of a simulated moving bed for enantioseparation of fluoxetine on New  $\beta$ -cyclodextrin columns. *Adsorption*, **9** (3), 213-223.
- Zhong, G., and Guiochon, G. (1996), Analytical solution for the linear ideal model of simulated moving bed Chromatography. *Chem. Eng. Sci.*, **51** (18), 4307-4319.

Received: May 29, 2009;  
 Revised: October 27, 2009;  
 Accepted: June 02, 2010.